Available online at www.sciencedirect.com
ScienceDirect
Geochimica et Cosmochimica Acta 71 (2007) 4557–4569
Geochimica et Cosmochimica Acta
www.elsevier.com/locate/gca

Iron/manganese ratio and manganese content in shield lavas from Ko'olau Volcano, Hawai'i

Shichun Huang [a,b,*], Munir Humayun [a,b], Frederick A. Frey [c]

[a] National High Magnetic Field Laboratory, Florida State University, 1800 E. Paul Dirac Drive, Tallahassee, FL 32310, USA
[b] Department of Geological Sciences, Florida State University, 108 Carraway Bldg., Tallahassee, FL 32306, USA
[c] Department of Earth, Atmospheric and Planetary Sciences, Massachusetts Institute of Technology, 77 Mass Ave., Cambridge, MA 02139, USA

Received 29 December 2006; accepted in revised form 9 July 2007; available online 6 August 2007

Abstract

Precise Fe/Mn ratios and MnO contents have been determined for basalts from the Hawaiian shields of Ko'olau and Kilauea by inductively coupled plasma mass spectrometry. It is well known that the youngest Ko'olau (Makapu'u-stage) shield lavas define a geochemical endmember for Hawaiian lavas in terms of CaO and SiO_2 contents and isotopic ratios of O, Sr, Nd, Hf, Pb, and Os. We find that their MnO content is also distinct. Despite the small range in MnO, 0.146 to 0.176 wt%, the precision of our data is sufficient to show that among unaltered Ko'olau lavas MnO content is correlated with Nd–Hf–Pb isotopic ratios, La/Nb and Al_2O_3/CaO elemental ratios, and contents of SiO_2, MgO and $Na_2O + K_2O$ adjusted for olivine fractionation. These trends are consistent with two-component mixing; one endmember is a SiO_2-rich, MnO-, and MgO-poor dacite or andesite melt, generated by low degree (10–20%) partial melting of eclogite. Since this low-MgO endmember (dacite or andesite melt) has very low FeO and MnO contents, mixing of high Fe/Mn dacite or andesite melt with a MgO-rich picritic melt, the other endmember, does not significantly increase the Fe/Mn in mixed magmas; consequently, Ko'olau and Kilauea lavas have similar Fe/Mn. We conclude that the high Fe/Mn in Hawaiian lavas relative to mid-ocean ridge basalt originates from the high MgO endmember in Hawaiian lavas.
© 2007 Elsevier Ltd. All rights reserved.

1. INTRODUCTION

Hawaiian volcanism has been extensively studied (e.g., Decker et al., 1987; Special Section of Hawai'i Scientific Drilling Project in J. Geophys. Res., Vol. 101, pp 11593–11864, 1996; Theme of Hawai'i Scientific Drilling Project in Geochem. Geophys. Geosyst. 2003). Currently there is debate about the role of eclogite (or garnet pyroxenite) in the source of Hawaiian shield lavas, presumably the Hawaiian plume (e.g., Hauri, 1996; Lassiter and Hauri, 1998; Norman and Garcia, 1999; Stracke et al., 1999; Takahashi and Nakajima, 2002; Pertermann and Hirschmann, 2003; Huang and Frey, 2005; Ren et al., 2005; Sobolev et al., 2005, 2007; Herzberg, 2006; Salters et al., 2006). In this debate, Ko'olau lavas play a central role. Among Hawaiian shields, Makapu'u-stage Ko'olau lavas are characterized by the highest SiO_2 content, La/Nb, $^{87}Sr/^{86}Sr$, $^{208}Pb^*/^{206}Pb^*$ and $^{18}O/^{16}O$, and lowest CaO content, $^{143}Nd/^{144}Nd$, $^{176}Hf/^{177}Hf$, and $^{206}Pb/^{204}Pb$. In detail, the olivine-adjusted SiO_2 contents in Ko'olau lavas are correlated with radiogenic isotopic ratios (Huang and Frey, 2005). These distinctive geochemical characteristics of Makapu'u-stage Ko'olau lavas have been proposed to be signatures of a dacite endmember, derived as partial melt of eclogite formed from recycled oceanic crust (MORB and sediments) in the Hawaiian plume (Frey and Rhodes, 1993; Frey et al., 1994; Hauri, 1996; Lassiter and Hauri, 1998; Blichert-Toft et al., 1999; Takahashi and Nakajima, 2002; Huang and Frey, 2005; Huang et al., 2005; Sobolev et al., 2005, 2007). However, the hypothesis that a dacite endmember is important in Hawaiian shield, especially

* Corresponding author. Fax: +1 850 644 0827.
E-mail addresses: huang@magnet.fsu.edu (S. Huang), humayun@magnet.fsu.edu (M. Humayun), fafrey@mit.edu (F.A. Frey).

0016-7037/$ - see front matter © 2007 Elsevier Ltd. All rights reserved.
doi:10.1016/j.gca.2007.07.013

Ko'olau, lavas has been questioned on petrological and geochemical grounds (e.g., Norman and Garcia, 1999; Stracke et al., 1999; Pertermann and Hirschmann, 2003; Pertermann et al., 2004; Salters et al., 2006; Sobolev et al., 2007).

We use Fe/Mn and MnO abundance to evaluate the role of eclogite in the source of Ko'olau lavas. Manganese, as MnO, is a minor element in igneous rocks. It is moderately incompatible during peridotite melting at high pressure (>3 GPa, Beattie, 1994; Walter, 1998; Humayun et al., 2004), and highly compatible during eclogite melting (Pertermann and Hirschmann, 2003). Consequently, partial melts of eclogite have lower MnO content than partial melts of peridotite. For example, adakites with >60% SiO_2, which are proposed as partial melts of the eclogitic portions of subducting slabs, have very low MnO content (0.05%) (Yogodzinski et al., 1995). Although MnO is routinely analyzed by X-ray fluorescence (XRF) and electron microprobe, mantle-derived melts (MORB and OIB) have a limited range in MnO content (typically 0.14–0.18%); therefore, MnO data are not typically used in assessing the petrogenesis of basaltic lavas. In principle, the presence of eclogite in the Hawaiian plume can be evaluated with precise data for Fe/Mn and MnO content. A complication is that fractionation and accumulation of olivine crystals modify the major element composition of Hawaiian lavas (e.g., Yang et al., 1996; Rhodes and Vollinger, 2004). However, during low pressure crystal fractionation, $D_{Mn}^{olivine/melt}$ is close to unity (e.g., Beattie, 1994; Ewart and Griffin, 1994). Consequently, MnO content of Hawaiian lavas is not very sensitive to olivine fractionation and accumulation.

Major element heterogeneity in the mantle is obviously important to mantle geochemistry; however it is also important to geophysics since composition and temperature control density and hence seismic wave velocity anomalies (e.g., Forte and Mitrovica, 2001). The density of the mantle is significantly controlled by Fe/Mg ratio, which is strongly fractionated during partial melting. To constrain variations in Fe abundance in the mantle, Humayun et al. (2004) and Qin and Humayun (submitted for publication) used the precise determination of Fe/Mn ratio in mantle-derived basalts. They reported a distinctly higher Fe/Mn ratio in Hawaiian lavas (66–71) compared with lavas of similar MgO content from Iceland (58–61). This excess Fe is of the same magnitude (±10%) as estimates based on mantle tomography (Forte and Mitrovica, 2001). Core-mantle interaction (Bennett et al., 1996; Brandon et al., 1998,1999) was proposed as the source of this excess Fe by Humayun et al. (2004) based on the assumption that the mantle source was peridotite. Alternatively, Sobolev et al. (2005, 2007) argued that the higher Fe/Mn in Hawaiian lavas reflects melting of olivine-free garnet pyroxenite, and pointed to the fact that the highest Fe/Mn in Hawaiian lavas are in two Ko'olau picrites, KOO-17A, and KOO-CF (Norman and Garcia, 1999; Humayun et al., 2004).

To evaluate these hypotheses, we report high precision Fe/Mn determined by sector field inductively coupled plasma mass spectrometry (ICP-MS) of 35 lavas cored by the Koolau Scientific Drilling Project (KSDP) and 24 Makapu'u-stage Ko'olau lavas (Haskins and Garcia, 2004; Huang and Frey, 2005). In addition, six Kilauea sample solutions that were analyzed by Humayun et al. (2004) were re-analyzed with these Ko'olau samples. The MnO content is calculated using Fe/Mn determined by ICP-MS and total iron as Fe_2O_3 content determined by XRF (Frey et al., 1994; Haskins and Garcia, 2004). Our objectives are to use MnO content to evaluate if a dacite endmember is important in Ko'olau lavas, and to evaluate if the high Fe/Mn in Hawaiian lavas is a result of partial melting of secondary garnet pyroxenite.

2. SAMPLES STUDIED

The Ko'olau Scientific Drilling Project deepened and cored a water well in the Ko'olau shield and recovered ~328 m of continuous core, which includes 103 lava flows (Haskins and Garcia, 2004). Ninety-one lava units from the KSDP drill core were analyzed for major and trace elements (Haskins and Garcia, 2004; Huang and Frey, 2005), and subsets of these samples were analyzed for Nd, Hf, and Pb isotopes (Salters et al., 2006; Fekiacova et al., in press). Geochemical studies indicate that most KSDP drillcore lavas have geochemical characteristics similar to Mauna Loa lavas, and the distinctive geochemical characteristics manifested by Makapu'u-stage Ko'olau lavas only occur in a subset of KSDP drillcore lavas (Haskins and Garcia, 2004; Huang and Frey, 2005; Salters et al., 2006). We selected 35 KSDP lavas and 24 Makapu'u-stage Ko'olau lavas for high precision Fe/Mn analysis; most of these samples have been analyzed for Nd, Hf, and Pb isotopes. In addition, in order to evaluate inter-shield difference in Fe/Mn, the six Kilauea solutions that were analyzed by Humayun et al. (2004) were re-analyzed with the new Ko'olau samples.

3. ANALYTICAL METHOD

About 40 mg of powdered sample of each Ko'olau lava was dissolved using ~5 ml HF–HNO_3 acids in 15 ml sealed Savillex® PFA beakers on a hotplate at ~200 °C. The solutions were dried, and residues were taken up in 1 ml concentrated HNO_3. This procedure was repeated twice. Then, the residues were taken up in 10 ml of 50% HCl. The sealed beakers were heated on a hotplate at 150 °C for ~12 h. Then the sample solutions were diluted with 1% HCl to form solutions with ~2–3 ppm Fe suitable for ICP-MS analysis. As mentioned in Humayun et al. (2004), because $FeCl_3$ is slightly volatile, complete drying of HCl solutions was avoided to prevent loss of Fe.

New Fe and Mn standard solutions were gravimetrically prepared by dissolving high purity Fe and Mn metals in HCl at the National High Magnetic Field Lab, Florida State University (FSU). Specifically, Fe stock solution (1000 ppm) was prepared by dissolving 0.39324 ± 0.00001 g (2σ) 99.998% pure Puratronic® metallic Fe wire in ~100 ml 25% HCl. Several drops of HNO_3 were added to enhance the reaction. After ~12 h, the resulting solution was diluted with 18.2 mega-ohm de-ionized H_2O, and the final solution weight was obtained gravimetrically. The resulting Fe concentration was 970.60 ± 0.06 ppm (2σ).

Manganese stock solution (1000 ppm) was prepared by dissolving 0.42706 ± 0.00002 g (2σ) g 99.98% pure Puratronic® metallic Mn turnings in ~100 ml 25% HCl. The reaction was complete in less than 10 min. Then, the solution was diluted with de-ionized H_2O to obtain a final Mn concentration of 1001.22 ± 0.07 ppm (2σ). A series of Fe–Mn standard solutions, with Fe/Mn ranging from 42 to 85, were gravimetrically prepared from these Fe and Mn stock solutions (Table 1) with a precision of ±0.01%, much better than our analytical uncertainty. These standard solutions were further diluted to make solutions with ~2 ppm Fe in 1% HCl for ICP-MS analysis. In contrast, the Fe–Mn standard solutions used by Humayun et al. (2004) were prepared from Spex Certiprep® high-purity Fe and Mn solutions at the University of Chicago; their concentrations are specified by the manufacturer as ±0.3%, valid only for one year from the date of certification. When compounded, the error on the Fe/Mn ratio is ±0.4% and this uncertainty approximately equals the analytical uncertainty. Further, the Spex Certiprep® solutions had been opened prior to their use in Fe/Mn standard preparation probably adding a systematic error to the uncertainty.

The Fe/Mn ratio was determined with a Finnigan Element 1 high-resolution inductively coupled plasma mass spectrometer (HR-ICP-MS) equipped with guard electrode (CD-1E), operated in low resolution ($R = 300$) mode. The standard and sample solutions were nebulized using ESI® 100 μL/min PFA nebulizer and an ESI® PFA spray chamber. The flat-topped peaks of $^{55}Mn^+$ and $^{57}Fe^+$ were monitored by electrically scanning the accelerating voltage (EScan mode) at 100 ms/peak over 10% of the mass window, with 600 sweeps of the mass spectrum at count rates of >20 million counts per second using a secondary electron multiplier operated in Analog mode. Polyatomic interferences, $^{37}Cl^{18}O^+$ and $^{38}Ar^{16}O^1H^+$ on $^{55}Mn^+$, $^{40}Ar^{16}O^1H^+$ on $^{57}Fe^+$, were corrected by measuring their intensities in a 1% HCl reference solution spaced within the analytical sequence. The interference corrections were about 1–3%, and the variations of interferences were ~10% throughout our typical analytical sequence (about 2 h). Measured $^{57}Fe^+/^{55}Mn^+$ intensity ratios in sample solutions were then converted to Fe/Mn abundance ratios using a calibration curve obtained on the Fe–Mn standard solutions (e.g., Fig. 1). Since $^{57}Fe^+/^{55}Mn^+$ intensity ratio is directly measured, any matrix effects on $^{57}Fe^+$ and $^{55}Mn^+$ intensities are cancelled out and do not affect the $^{57}Fe^+/^{55}Mn^+$ intensity ratio. The measured Fe/Mn is reported in Table 2, and 33 measurements of BHVO-1 during the course of this study give an average of 64.75 ± 0.39 (2σ), which correspond to a relative uncertainty of 0.6%. Then MnO content of each Ko'olau sample was calculated using Fe/Mn determined by ICP-MS (0.6%, 2σ) and reported total iron content as Fe_2O_3 determined by XRF (0.5%, 2σ; Frey et al., 1994; Rhodes, 1996; Haskins and Garcia, 2004), and is listed in Tables 2a and 2b. Results for Kilauea samples are given in Table 2c. Using error propagation, the estimated relative uncertainty of MnO content is 0.8% (2σ).

Calibration curves of the new FSU Fe–Mn standard solutions (this study) and new analyses of the Chicago Fe–Mn standard solutions used by Humayun et al. (2004) are shown in Fig. 1a. The calibration curve of the Chicago Fe–Mn standard solutions is slightly offset from the calibration curve of the new FSU Fe–Mn standard solutions. The measured Fe/Mn in FSU Fe–Mn standard solutions are

Table 1
Fe/Mn ratios and Mn and Fe concentrations (ppm) in gravimetrically prepared FSU standard solutions

Fe/Mn gravimetric	[Mn] ppm	[Fe] ppm
85.632 ± 9	1.8515	158.6
75.325 ± 8	1.8715	141.0
69.858 ± 8	1.8283	127.7
66.622 ± 7	1.8477	123.1
65.661 ± 7	1.8813	123.5
64.464 ± 7	1.8406	118.7
63.409 ± 7	1.8771	119.0
62.273 ± 7	1.8320	114.1
59.114 ± 6	1.8882	111.6
53.459 ± 6	1.8376	98.24
42.288 ± 6	1.9630	83.01

The relative uncertainties on the Mn and Fe concentrations are 0.01% (2σ).

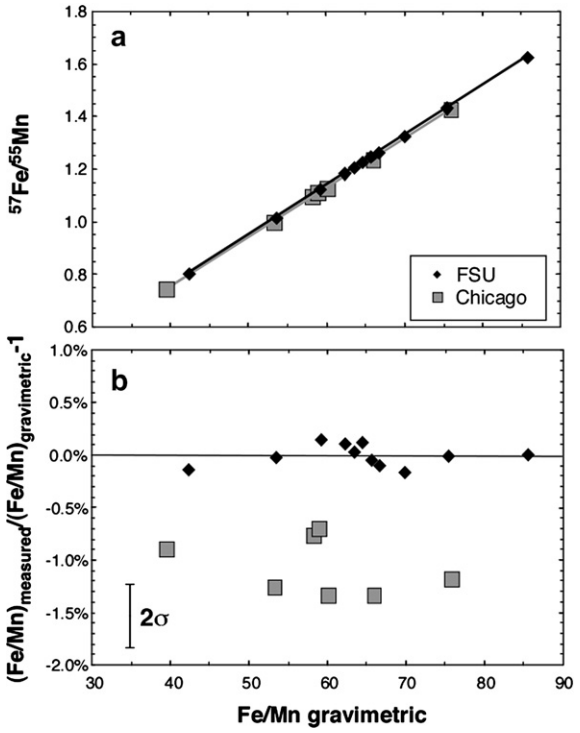

Fig. 1. (a) Measured $^{57}Fe/^{55}Mn$ intensity ratios versus their gravimetric Fe/Mn weight ratios for separate Fe–Mn standard solutions prepared at Florida State University and the University of Chicago. The calibration curve of the Chicago standard solutions is slightly offset from that of the FSU standard solutions. (b) The difference between the measured and the gravimetric values of the same sets of standard solutions (relative to the FSU standard set). For comparison, the external reproducibility of Fe/Mn is 0.6% (2σ) estimated on 33 measurements of a BHVO-1 solution, and is shown as an error bar in (b).

Table 2a
MgO and total iron (as Fe_2O_3) contents (XRF), Fe/Mn, and MnO content (ICP-MS) in KSDP Ko'olau lavas[a]

Unit	MgO (%)	Fe_2O_3 total (%)	Fe/Mn	MnO (%)
1	15.42	11.72	67.12	0.158
6	15.07	11.53	66.97	0.156
8	11.53	11.86	65.76	0.163
9	9.19	11.34	64.10	0.160
15	9.49	12.28	66.32	0.167
17	7.51	12.05	64.91	0.168
20	13.66	12.28	68.42	0.162
24	7.18	11.64	64.14	0.164
25	7.26	11.70	64.77	0.163
27	6.88	11.34	63.86	0.160
29	12.81	12.42	64.13	0.175
34	9.64	12.13	64.93	0.169
37	8.07	12.00	64.48	0.168
38	7.60	12.11	63.32	0.173
41	7.38	12.34	64.42	0.173
44	7.35	12.24	64.30	0.172
46	7.58	11.68	65.15	0.162
48	6.87	11.53	63.96	0.163
49	7.41	11.79	65.08	0.164
50	9.79	11.82	64.90	0.165
51	7.56	11.64	64.35	0.163
53	12.02	11.90	65.72	0.164
54	6.95	11.80	62.71	0.170
57	7.37	11.89	65.80	0.163
61	7.34	11.71	64.68	0.163
62	8.68	11.97	64.58	0.167
63	6.90	11.66	64.09	0.164
66	8.60	11.48	64.13	0.162
67	8.78	11.35	63.56	0.161
68	10.09	11.69	64.87	0.163
71	8.17	11.56	62.55	0.167
74	7.23	11.44	64.64	0.160
76	9.62	12.44	63.92	0.176
85	8.50	12.18	73.02	0.151
88	13.02	12.46	45.22	0.249

[a] MgO and total iron (as Fe_2O_3) contents are from Haskins and Garcia (2004). MnO content is calculated using XRF total iron (as Fe_2O_3) content and ICP-MS Fe/Mn.

Table 2b
MgO and total iron (as Fe_2O_3) contents (XRF), Fe/Mn, and MnO content (ICP-MS) in Makapu'u-stage Ko'olau lavas[a]

Sample	MgO (%)	Fe_2O_3 total (%)	Fe/Mn	MnO (%)
KOO-1	7.14	11.00	65.44	0.152
KOO-7	6.99	11.69	66.08	0.160
KOO-8	7.25	11.58	67.22	0.156
KOO-10	10.71	11.55	65.41	0.159
KOO-15	7.08	11.48	65.81	0.158
KOO-17	8.86	11.17	64.70	0.156
KOO-17A			68.77	
KOO-17A DUP			68.22	
KOO-17A ave.	21.54	12.69	68.50	0.167
KOO-19	6.58	10.86	66.11	0.148
KOO-21	9.26	11.09	66.72	0.150
KOO-24	8.81	11.53	65.68	0.159
KOO-32	9.21	11.04	64.48	0.155
KOO-48	6.84	11.32	65.52	0.156
KOO-49	10.15	11.86	67.35	0.159
KOO-55			70.51	
KOO-55 DUP			71.84	
KOO-55 ave.	8.35	11.69	71.18	0.148
KOO-55D			73.36	
KOO-55D DUP			74.42	
KOO-55D ave.	10.44	11.98	73.89	0.146
KOO-CF			70.06	
KOO-CF DUP			70.31	
KOO-CF ave.	15.37	12.08	70.19	0.155
KM-1	13.57	11.83	66.72	0.160
KM-3	12.64	11.13	64.75	0.155
OH-21	6.83	11.13	66.89	0.150
OH-22	6.76	11.46	68.42	0.151
OH-24	6.79	10.99	68.46	0.145
OH-25	7.04	11.88	70.50	0.152
OH-26	6.72	10.97	66.22	0.150
OH-27	6.28	10.83	67.80	0.144

[a] MgO and total iron (as Fe_2O_3) contents of KOO-CF are from Norman and Garcia (1999), others are from Frey et al. (1994). MnO content is calculated using XRF total iron (as Fe_2O_3) content and ICP-MS Fe/Mn. Duplicate analyses were measured on separate dissolutions.

within 0.2% of their gravimetric Fe/Mn values, and the measured Fe/Mn in Chicago Fe–Mn standard solutions are systematically lower than their gravimetric Fe/Mn values by ~1% (Fig. 1b). This difference is also indicated in reported Fe/Mn for USGS standard BHVO-2. Humayun et al. (2004) reported 66.14 (0.5%, 2σ) for BHVO-2, and our six measurements of BHVO-2 during the course of this study give an average of 65.25 (0.6%, 2σ) (Table 2c). Consequently, in this paper the Fe/Mn measurements reported by Humayun et al. (2004) are normalized to the FSU Fe–Mn standard solutions using the reported BHVO-2 values.

4. RESULTS AND DISCUSSIONS

At a given MgO content, Ko'olau lavas have higher Fe/Mn than MORB (53–57) and Icelandic (58–61) lavas, and the Fe/Mn range in Ko'olau lavas is similar to that in the five Hawaiian shields (Fig. 2). In detail, some

Table 2c
MgO and total iron (as FeO) contents (XRF), Fe/Mn, and MnO content (ICP-MS) in Kilauea lavas[a]

Sample	MgO (%)	FeO total (%)	Fe/Mn	MnO (%)
KIL-1-7			67.74	
KIL-1-7 DUP			66.78	
KIL-1-7 ave.	15.97	11.14	67.26	0.166
KIL-1-10	18.24	11.17	67.45	0.166
KIL-1-18	13.80	11.33	66.84	0.170
KIL-2-1	20.66	11.31	67.44	0.168
KIL-1840-1	14.27	11.22	66.13	0.170
KIL-93-1489	8.90	11.22	64.56	0.174
BHVO-2	7.23	11.10	65.25	0.171
BHVO-1	7.09	10.95	64.75	0.170

[a] MgO and total iron as FeO contents are from Norman and Garcia (1999). MnO content is calculated using XRF total iron as FeO content and ICP-MS Fe/Mn. Duplicate analyses were measured on separate dissolutions.

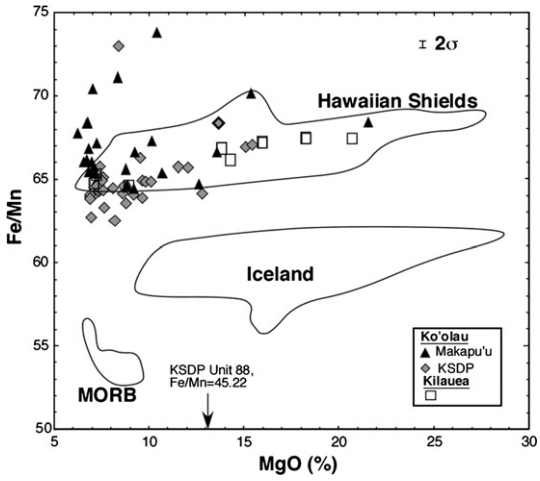

Fig. 2. MgO (%) versus Fe/Mn in Ko'olau and Kilauea lavas. Fields for published data of Hawaiian shield lavas (Humayun et al., 2004), and MORB and Icelandic lavas (Qin and Humayun, submitted for publication) are shown for comparison. The MORB field (Fe/Mn ~ 53–57) is defined by 14 samples from Pacific, Indian and Atlantic oceans, and the Icelandic field (Fe/Mn ~ 58–61) is defined by 19 Holocene lavas from Reykjanes rift (western volcanic zone), Theistareykir (northern volcanic zone) and Skridufell (central volcanic zone). At a given MgO content, KSDP Ko'olau lavas have similar or lower Fe/Mn than Kilauea lavas, and Makapu'u-stage Ko'olau lavas have similar or higher Fe/Mn than Kilauea lavas.

Ko'olau lavas have Fe/Mn > 70, and plot above the Hawaiian field. Importantly, at a given MgO content, Makapu'u-stage Ko'olau lavas have similar or slightly higher Fe/Mn than KSDP Ko'olau lavas, and KSDP Ko'olau lavas have Fe/Mn similar to, or lower than Kilauea lavas (Fig. 2).

4.1. Alteration effect on Fe/Mn

In addition to Loss on Ignition (LOI), the abundance ratio of K_2O/P_2O_5 is a good alteration indicator for subaerially erupted Hawaiian lavas, with altered Hawaiian lavas exhibiting unusually high or low K_2O/P_2O_5 (e.g., Feigenson et al., 1983; Frey et al., 1991, 1994; Yang et al., 1996; Huang and Frey, 2003; Haskins and Garcia, 2004). In this paper, we arbitrarily define lavas with $1.3 < K_2O/P_2O_5 < 2.0$ as unaltered lavas, and lavas with $K_2O/P_2O_5 < 1.3$ or >2.0 as altered lavas. The effect of subaerial alteration on Fe/Mn is indicated in Fig. 3a. Ko'olau lavas with $1.3 < K_2O/P_2O_5 < 2.0$ have Fe/Mn of 62.71–68.42. In contrast, Ko'olau lavas with $K_2O/P_2O_5 < 1.3$ or >2.0 have Fe/Mn ranging from 45.22 to 73.89, and most altered Ko'olau lavas tend to have higher Fe/Mn than unaltered Ko'olau lavas. The two Makapu'u-stage Ko'olau picrites, KOO-17A and KOO-CF, which were analyzed by Humayun et al. (2004), have K_2O/P_2O_5 of 0.5 and 2.2, respectively, and they have higher Fe/Mn than unaltered Ko'olau lavas (Fig. 3a). KSDP Unit 88 has Fe/Mn of 45.22, the lowest value in all analyzed Hawaiian lavas. This sample is highly altered and has a LOI of 3.65%, and K_2O/P_2O_5 of 1.1 (Haskins and Garcia, 2004). At a given MgO content, altered Makapu'u-stage Ko'olau lavas tend to have slightly higher

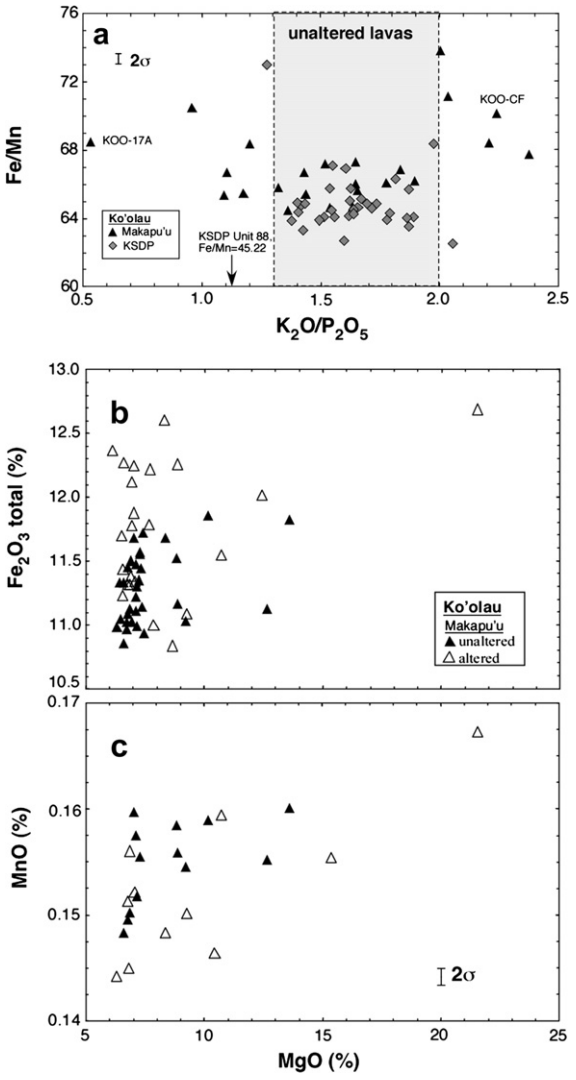

Fig. 3. (a) K_2O/P_2O_5 versus Fe/Mn in Ko'olau lavas. The grey field with dashed lines highlights unaltered lavas with $1.3 < K_2O/P_2O_5 < 2.0$. Altered lavas with $K_2O/P_2O_5 < 1.3$ or >2.0 have more scattered (generally higher) Fe/Mn than unaltered lavas. (b,c) MgO (%) versus total iron as Fe_2O_3 (%) and MnO (%) in Makapu'u stage Ko'olau lavas. Unaltered lavas have $1.3 < K_2O/P_2O_5 < 2.0$, and altered lavas have $K_2O/P_2O_5 < 1.3$ or >2.0. Clearly, altered Makapu'u-stage Ko'olau lavas tend to have higher total iron as Fe_2O_3 content than unaltered ones. However, our limited MnO dataset does not show an obvious difference between altered and unaltered Makapu'u-stage Ko'olau lavas. Data source: total Fe_2O_3 from Frey et al. (1994), MnO from this study.

total iron as Fe_2O_3 content than unaltered Makapu'u-stage Ko'olau lavas (Fig. 3b). Our limited MnO dataset does not show obvious difference between altered and unaltered Makapu'u-stage Ko'olau lavas (Fig. 3c); however, the altered KSDP lava Unit 88 has very high MnO content of 0.249%, which is significantly higher than other Hawaiian lavas (0.144–0.176%, Table 2). To be conservative, in the following discussion, we only focus on lavas with $1.3 < K_2O/P_2O_5 < 2.0$ and LOI < 0.8%.

4.2. Inter- and intra-shield MnO variation in Hawaiian lavas

Although lavas from different Hawaiian shields have similar Fe/Mn (Fig. 2), there are important inter- and intra-shield differences in contents of total iron as Fe_2O_3 and MnO. In a MgO-total iron plot, Kilauea lavas and Ko'olau lavas show two subparallel, nearly horizontal fields, with Kilauea lavas having higher total iron content ($12.6\% \pm 1.0$, 2σ) than unaltered ($1.3 < K_2O/P_2O_5 < 2.2$, LOI $< 0.8\%$) Ko'olau lavas ($11.7\% \pm 1.0$, 2σ) (Fig. 4a). In detail, among Ko'olau lavas, unaltered Makapu'u-stage Ko'olau lavas have lower total iron content ($11.3\% \pm 0.6$, 2σ) than KSDP Ko'olau lavas ($11.9\% \pm 0.8$, 2σ). Note that major elements of Ko'olau lavas and majority of the Kilauea lavas were analyzed using the same XRF facility at the University of Massachusetts (Frey et al., 1994; Chen et al., 1996; Haskins and Garcia, 2004), so this total iron difference between different lava suites does not reflect inter-lab bias. Ko'olau lavas do not form an obvious trend in a MgO–MnO plot, and show considerable scatter in MnO content at a given MgO content (Fig. 4b). In contrast, eight Kilauea lavas form a nearly horizontal trend in a MgO–MnO plot. At a given MgO content, Kilauea lavas have higher MnO content than KSDP Ko'olau lavas, and Makapu'u-stage Ko'olau lavas have lower MnO content than KSDP Ko'olau lavas.

The nearly horizontal MgO–MnO trend of Kilauea lavas (Fig. 4b) probably reflects olivine fractionation and accumulation, implying that $D_{Mn}^{olivine/melt}$ is close to unity during low pressure crystal fractionation (e.g., Beattie, 1994; Ewart and Griffin, 1994). What causes the scatter of MnO content in Ko'olau lavas? MnO contents of Ko'olau lavas are correlated with Nd–Hf–Pb isotopes and La/Nb (Fig. 5), implying mantle source control. Since most Hawaiian shield lavas experienced low pressure olivine fractionation or accumulation, following Huang and Frey (2005), we adjusted the major element composition (SiO_2, total FeO and MgO) of Ko'olau lavas to be in equilibrium with Fo_{90} olivine, by adding or subtracting equilibrium olivine in 0.1 wt% steps assuming $(Fe/Mg)_{olivine}/(Fe/Mg)_{melt} = 0.30$. For simplicity, in the following discussion we use SiO_2*, MgO*, and $(Na_2O + K_2O)$* contents representing olivine-adjusted contents of SiO_2, MgO, and $Na_2O + K_2O$. After olivine adjustment, within Ko'olau lavas SiO_2* and MgO* contents are correlated with measured MnO content (Figs. 6a and b). Note that, since MnO content is not very sensitive to olivine fractionation and accumulation (Fig. 4b), we use the measured MnO content in Fig. 6. It can be seen in Fig. 6b that MnO content is correlated with MgO* content, even though MnO content does not correlate with measured MgO content (Fig. 4b). The linear correlations between MnO content and SiO_2*, MgO* contents, Nd–Hf–Pb isotopic ratios and La/Nb (Figs. 5 and 6a and b) in Ko'olau lavas imply two-endmember mixing with the enriched Hawaiian endmember (high SiO_2 content, $^{208}Pb^*/^{206}Pb^*$, La/Nb and low MgO content, $^{143}Nd/^{144}Nd$, $^{176}Hf/^{177}Hf$, $^{206}Pb/^{204}Pb$), known as the Ko'olau (Makapu'u) endmember, having low MnO content (<0.15%).

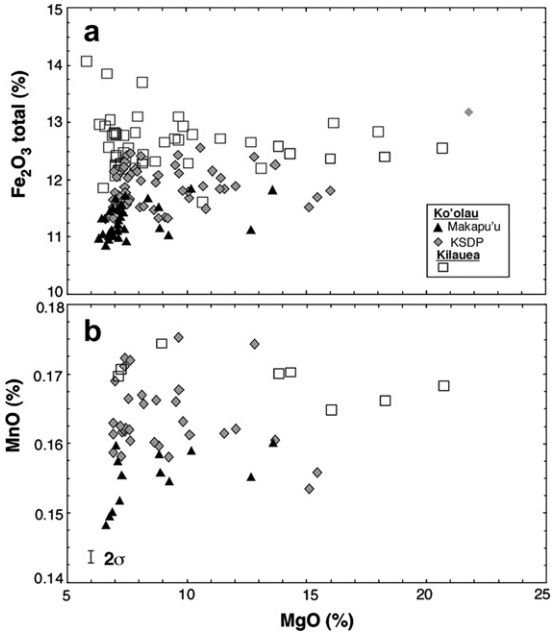

Fig. 4. MgO versus total iron as Fe_2O_3 and MnO contents (%) for Ko'olau and Kilauea lavas. Only lavas with $1.3 < K_2O/P_2O_5 < 2.0$ and LOI $< 0.8\%$ are plotted. Note the lower MnO content of the Makapu'u-stage Ko'olau lavas. Data source: Kilauea (Chen et al., 1996; Norman and Garcia, 1999; Humayun et al., 2004); Ko'olau (Frey et al., 1994; Haskins and Garcia, 2004; this study).

The eight Kilauea lavas form vertical trends in plots of MnO vs $^{206}Pb/^{204}Pb$ and $^{208}Pb^*/^{206}Pb^*$ (Figs. 5c and d) and horizontal trends in plots of MnO vs SiO_2* and $(Na_2O + K_2O)$* (Figs. 6a and c). The different trends formed by lavas from Kilauea, a Kea-trend volcano, and Ko'olau, a Loa-trend volcano, may reflect a Loa-Kea geochemical difference. Important geochemical differences in major and trace elements, and isotopic ratios between Loa-trend and Kea-trend lavas have been documented (e.g., Lassiter et al., 1996; Abouchami et al., 2005; Huang et al., 2005). Specifically, Loa-trend lavas sampled variable amounts of the Ko'oalu (Makapu'u) endmember that is absent in Kea-trend lavas (Huang et al., 2005). However, more MnO data on different Hawaiian shields are required to determine if there are systematic differences in MnO content between Loa- and Kea-trend volcanoes. In this paper, we will focus on the origin of the low-MnO Ko'olau (Makapu'u) endmember.

What is the origin of the Ko'olau (Makapu'u) endmember? High SiO_2 content is a distinct geochemical characteristic of the Ko'olau (Makapu'u) endmember, which has been proposed to reflect a SiO_2-rich melt derived from eclogite (Hauri, 1996; Huang and Frey, 2005). Huang and Frey (2005) discussed in detail the pros and cons of this proposal. Below we summarize the important issues.

Frey and Rhodes (1993) and Frey et al. (1994) noted that Makapu'u-stage Ko'olau lavas have higher SiO_2 content than Kilauea lavas. Hauri (1996) showed that there are important inter-shield correlations between major element contents and isotopic ratios. Specifically, the average SiO_2 and CaO contents of each Hawaiian shield, adjusted to be in equilibrium with Fo_{90} olivine, are correlated with

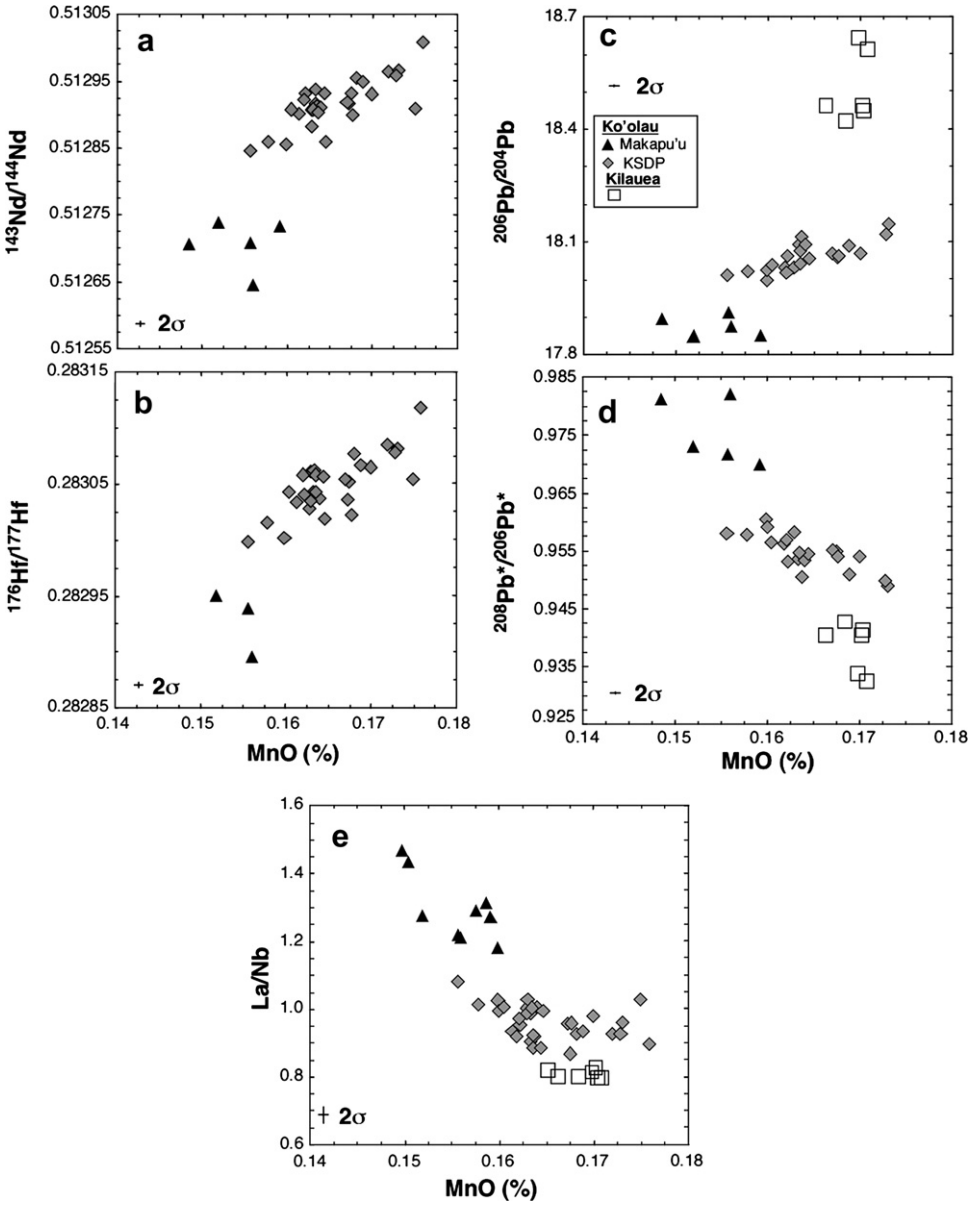

Fig. 5. MnO content (%) versus $^{143}Nd/^{144}Nd$, $^{176}Hf/^{177}Hf$, $^{206}Pb/^{204}Pb$, $^{208}Pb^*/^{206}Pb^*$, and La/Nb in Ko'olau and Kilauea lavas. $^{208}Pb^*/^{206}Pb^*$ represents the time-integrated $^{232}Th/^{238}U$ since the Earth formation, and is defined as $[(1^{208}Pb/^{204}Pb)_{sample} - 29.475]/[(^{206}Pb/^{204}Pb)_{sample} - 9.307]$ (Galer and O'Nions, 1985). MnO content is highly correlated with Nd–Hf–Pb isotopic ratios and La/Nb. Since $^{87}Sr/^{86}Sr$ and $^{143}Nd/^{144}Nd$ are not available for Kilauea picrites (Norman and Garcia, 1999), they are not shown in (a and b). Ko'olau: Nd and Hf isotopic data are from Roden et al. (1994); Lassiter and Hauri (1998); Blichert-Toft et al. (1999) and Salters et al. (2006); Pb isotopic data are from Roden et al. (1994); Lassiter and Hauri (1998) and Fekiacova et al. (in press); La/Nb data are from Frey et al. (1994) and Huang and Frey (2005). Kilauea: Pb isotopic data and La/Nb are from Norman and Garcia (1999).

their average isotopic ratios, with Makapu'u-stage Ko'olau lavas defining the high SiO_2 endmember. Huang and Frey (2005) showed that within the Ko'olau shield the SiO_2* content is correlated with Nd–Hf–Pb isotopic ratios. In addition, Garcia (2002) and Sobolev et al. (2005) found that olivines from the Ko'olau shield have higher Ni content than olivines from other Hawaiian shields. Consequently, the Ko'olau endmember is characterized by relatively high SiO_2 and $K_2O + Na_2O$ contents and low CaO content that are correlated with isotopic ratios ($^{87}Sr/^{86}Sr$, $^{143}Nd/^{144}Nd$, $^{176}Hf/^{177}Hf$ and $^{206}Pb/^{204}Pb$, $^{208}Pb^*/^{206}Pb^*$, $^{187}Os/^{188}Os$, and $\delta^{18}O$); also this component has a strong residual garnet signature, i.e., Makapu'u-stage Ko'olau lavas have relatively low Sc and Yb abundances and high La/Yb, and olivines with high Ni contents. The high SiO_2 content in Makapu'u-stage Ko'olau lavas was originally proposed to reflect a lower magma segregation pressure for Ko'olau lavas (Frey et al., 1994). However, Hauri (1996) showed that the high SiO_2 content in Makapu'u-stage Ko'olau lavas requires magma segregation at depths of 30–45 km, thinner

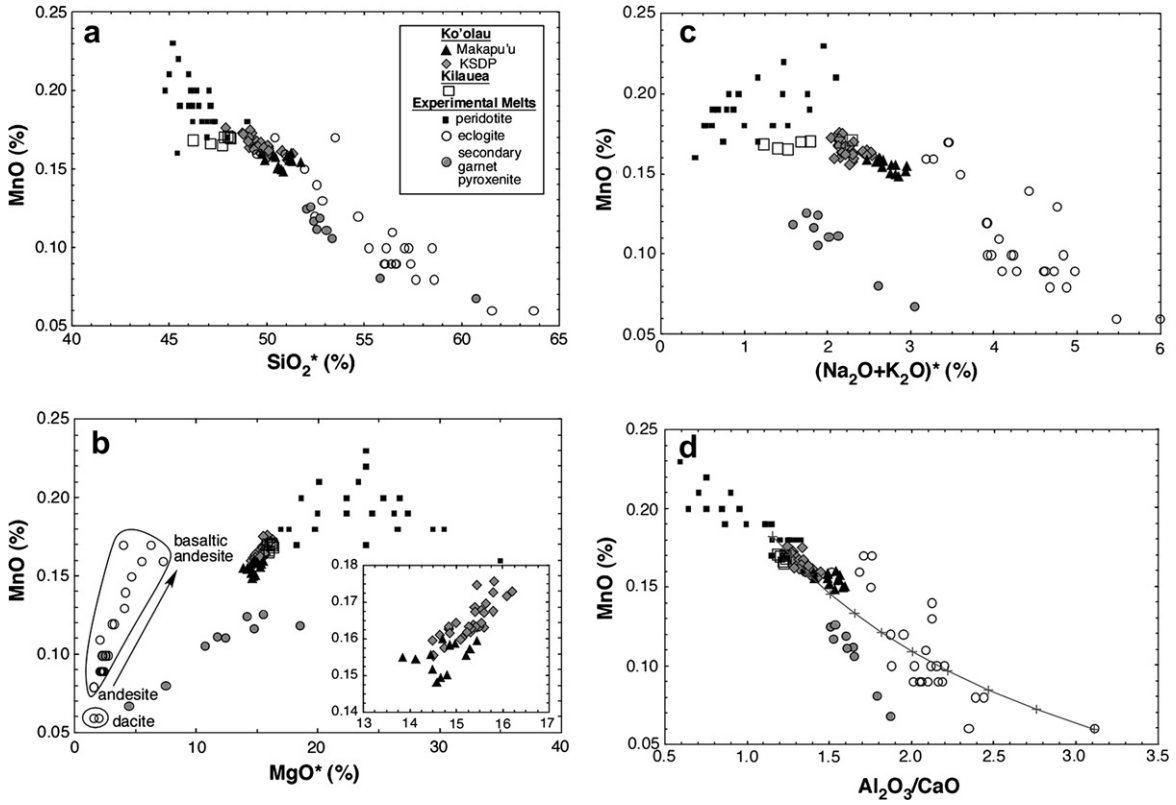

Fig. 6. SiO_2*, MgO*, $(Na_2O + K_2O)$*, and Al_2O_3/CaO versus MnO content in Ko'olau and Kilauea lavas. Star values represent olivine-adjusted major element compositions. See text for details. Since MnO content is not very sensitive to olivine fractionation and accumulation (Fig. 4b), measured MnO content is used in this figure. Experimental melts of garnet peridotite (Walter, 1998), MORB-like eclogite (Pertermann and Hirschmann, 2003) and the secondary garnet pyroxenite (Sobolev et al., 2005, 2007) are plotted for comparison. In detail, partial melts of eclogite range from dacite to andesite to basaltic andesite. The inset in (b). shows the MgO*–MnO correlation of Ko'olau lavas in detail. In (d), a mixing line, with an increment of 10%, between a picrite melt and a dacite melt is shown, and it explains the negative trend of Ko'olau lavas. Model details are in Table 3.

than Hawaiian lithosphere (Li et al., 2004). Also, Hauri (1996) showed that Hawaiian primary magmas, in general, have much higher FeO content than the experimental melts of peridotite at low pressure. That is, the estimated primary magma compositions of Hawaiian shield lavas, especially Ko'olau lavas, are not in equilibrium with garnet peridotite. Moreover Eggins (1992) and Wagner and Grove (1998) experimentally showed that the estimated Kilauea primary magma compositions have SiO_2 content too high to be in equilibrium with garnet peridotite.

An alternative idea, melt-mantle reaction, was proposed to increase the SiO_2 content in Hawaiian shield lavas (Eggins, 1992; Wagner and Grove, 1998; Stolper et al., 2004). To explain the SiO_2 difference between the two SiO_2 groups of Mauna Kea lavas, Stolper et al. (2004) proposed that high-SiO_2 group lavas were formed by crystallization of ~12% olivine from, and assimilation of ~12% orthopyroxene and ~8% clinopyroxene by, low-SiO_2 group lavas. Since this reaction involves <20% orthopyroxene and clinopyroxene, phases with low abundances of Nd, Hf, and Pb relative to basaltic melt, it is unlikely that melt-mantle reaction can modify the isotopic ratios of Nd, Hf, and Pb in melt. Consequently, melt-mantle reaction cannot explain the major element content-isotope correlations observed by Hauri (1996) and Huang and Frey (2005). Further, this melt-mantle reaction slightly increases CaO content with increasing SiO_2 content in the melt (Fig. 14d of Stolper et al., 2004), which cannot explain the coupled low-CaO and high-SiO_2 in Makapu'u-stage Ko'olau lavas (Frey et al., 1994; Haskins and Garcia, 2004; Huang and Frey, 2005).

Hauri (1996) and Huang and Frey (2005) proposed that the distinctive geochemical characteristics of the Ko'olau endmember are signatures of a dacite melt, generated by small degree (10–20%) partial melting of eclogite, formed from recycled oceanic crust (MORB and sediments). This dacite melt must be mixed with picritic melts generated by garnet peridotite melting to explain the distinct compositions of Hawaiian shield lavas. Since SiO_2-rich dacite melts are likely to react with surrounding peridotite, Sobolev et al. (2005) suggested a two-stage model. In the first stage, eclogite partially melts at great depth (~150 km) to generate SiO_2-rich dacite melt, which reacts with surrounding peridotite, replaces olivine with clinopyroxene, and forms an olivine-free secondary garnet pyroxenite. In the second stage, partial melts (~40% degree of partial melting) of this secondary garnet pyroxenite are formed with high SiO_2 (>49%) and Ni contents, which are then mixed with melts

from garnet peridotite to form the Hawaiian shield lavas. However, Salters et al. (2006) argued that if the dacite endmember, with Mg# ~35, is important in Hawaiian lavas, it is incorrect to adjust magma compositions to be in equilibrium with a common olivine composition (Fo_{90}). Therefore, Salters et al. (2006) argued that the observed correlations between major element content and isotopic ratios (Hauri, 1996; Huang and Frey, 2005) are artifacts, and they argued against the presence of eclogite in the Hawaiian plume. However, dacite melts have much lower FeO and MgO contents than picrite melts (e.g., Yaxley and Green, 1998; Pertermann and Hirschmann, 2003). Consequently, adding a large amount (up to 30%) of dacite melt into picrite melt does not significantly change the olivine composition in equilibrium with the mixed melts (Table 3). This result is consistent with abundant olivine phenocrysts, up to Fo_{90}, in Ko'olau lavas (Garcia, 2002; Haskins and Garcia, 2004).

Are the linear correlations between MnO content and SiO_2*, MgO* contents, Nd–Hf–Pb isotopic ratios, and La/Nb (Figs. 5 and 6a and b) in Ko'olau lavas consistent with a dacite melt contributing to Ko'olau lavas? Specifically, is the low MnO content identified in the Ko'olau (Makapu'u) endmember consistent with an eclogite origin? MnO is slightly incompatible in garnet peridotite melting at high pressure (>3 GPa), but it is compatible in partial melting of eclogite and garnet pyroxenite (Fig. 7a). High-pressure (2–3 GPa) experiments on partial melting of MORB-like eclogite show that low degree dacite melts have low MgO and MnO contents, and high SiO_2 and $Na_2O + K_2O$ contents (Pertermann and Hirschmann, 2003; Figs. 6 and 7). This experimental result is consistent with the low MnO content (0.05%) in adakites, which are suggested to be low degree partial melts derived from subducting slabs containing eclogite (Yogodzinski et al., 1995). In addition, new experiments show that partial melts of a secondary garnet pyroxenite composition proposed by Sobolev et al. (2005) also yield low MgO and MnO, and high SiO_2 contents (Sobolev et al., 2007; Fig. 6). In contrast, experimental partial melts of garnet peridotite at high pressure (>3 GPa) have high MgO and MnO contents and low SiO_2 content; they cannot be the Ko'olau (Makapu'u) endmember (Figs. 6 and 7). The positive MnO–MgO* trend in Fig. 6b suggests that the Ko'olau (Makapu'u) endmember should be similar to the dacite and andesite melts generated by low

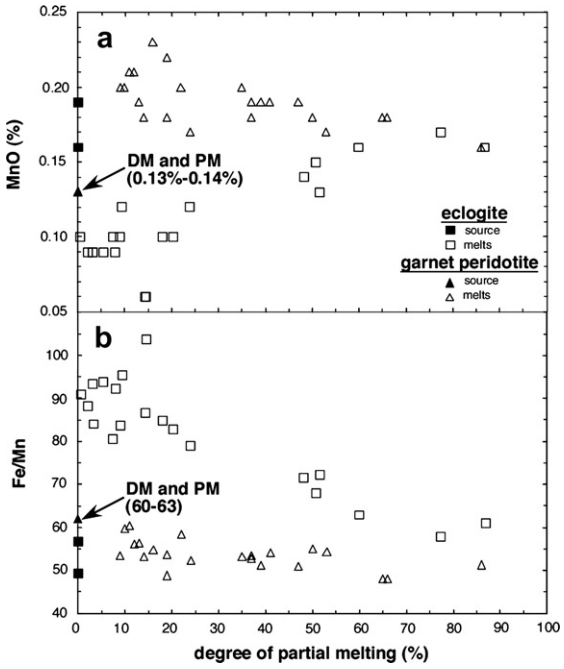

Fig. 7. MnO and Fe/Mn in experimental melts of garnet peridotite and MORB-like eclogite versus degree of partial melting. MnO is compatible in partial melting of MORB-like eclogite, but it is slightly incompatible in partial melting of garnet peridotite. Low degree partial melting of MORB-like eclogite significantly increases Fe/Mn in the melts; in contrast, partial melting of garnet peridotite only slightly decreases Fe/Mn in the melts. Depleted mantle (DM) and primitive mantle (PM) estimates from McDonough and Sun (1995), Salters and Stracke (2004) and Workman and Hart (2005) are shown for comparison. Peridotite and eclogite sources, and experimental melt compositions are from Walter (1998) and Pertermann and Hirschmann (2003).

Table 3
Mixing model parameters

	SiO_2 (%)	Al_2O_3 (%)	Total FeO (%)	MnO (%)	MgO (%)	CaO (%)	Fe/Mn	Equilibrium olivine Fo[f]
Picrite endmember[a]	46.84	11.23	9.60	0.18	19.64	9.69	52.8	92
Hypothetical Fe-rich picrite endmember[b]	46.84		11.70	0.18			64.4	
Dacite endmember[c]	63.64	15.35	5.18	0.06	1.54	4.93	86.7	64
Sobolev high-SiO_2 endmember[d]	53.03	13.77	8.13	0.11	12.33	8.58	73.4	90
30% dacite + 70% picrite[e]	51.88	12.47	8.27	0.14	14.21	8.26	57.0	91

[a] Average composition of melts generated at 3-4 GPa in Walter (1998).
[b] Since SiO_2 content in partial melts of peridotite is not very sensitive to source composition (Hirose and Kushiro, 1993), we assume that the hypothetical picrite melt of an Fe-rich peridotite has SiO_2 of 46.84% and MnO of 0.18%, the same as in those the experimental picrite melt, and FeO of 11.7% and Fe/Mn of 64, similar to those in Hawaiian lavas.
[c] Melt composition of Run A200K (Pertermann and Hirschmann, 2003).
[d] High SiO_2 endmember from Sobolev et al. (2007).
[e] Mixture of 30% dacite endmember and 70% picrite endmember.
[f] Equilibrium olivine is calculated assuming $(Fe/Mg)_{olivine}/(Fe/Mg)_{melt} = 0.3$.

degree (10–20%) partial melting of eclogite (Huang and Frey, 2005), or the partial melts of the secondary garnet pyroxenite (Sobolev et al., 2005, 2007).

Recycled ferromanganese sediments (Fe/Mn ~ 1–31) in the Hawaiian plume, which have been proposed as a possible component explaining the radiogenic $^{186}Os/^{188}Os$ observed in Hawaiian lavas (Ravizza et al., 2001), could significantly affect the MnO content and Fe/Mn in Hawaiian lavas. Since Tl isotopic ratios are very sensitive to the presence of even small amounts of ferromanganese sediments, Nielsen et al. (2006) constrained the amount of ferromanganese sediments in the Hawaiian plume at less than 30 ppm by mass from Tl isotopic ratios in Hawaiian lavas. They determined that the effect of ferromanganese sediment on MnO content, Fe/Mn or Os isotopic ratios in Hawaiian lavas is negligible.

4.3. Effect of eclogite endmember on Fe/Mn

Humayun et al. (2004) noted that Hawaiian lavas have higher Fe/Mn than MORB and Icelandic lavas (Fig. 2). Assuming an olivine-dominated source for Hawaiian shield lavas, Humayun et al. (2004) proposed that the high Fe/Mn is an outer core signature. However, partial melts of an olivine-free source, eclogite or the secondary garnet pyroxenite, also have elevated Fe/Mn (Fig. 7b; Pertermann and Hirschmann, 2003; Humayun et al., 2004; Sobolev et al., 2007). For example, the low degree (10–20%) partial melts of eclogite have Fe/Mn > 80, and ~50% partial melts have Fe/Mn of 60–70 (Fig. 7b; Pertermann and Hirschmann, 2003). Consequently, Sobolev et al. (2005, 2007) proposed that the high Fe/Mn in Hawaiian lavas is the result of sampling a secondary garnet pyroxenite component. Below we evaluate this argument.

In Fig. 8, SiO_2* content is plotted against Fe/Mn in Ko'olau and Kilauea lavas. Since Fe/Mn is not very sensitive to olivine fractionation and accumulation (Fig. 2), we plot measured Fe/Mn in Fig. 8. Ko'olau and Kilauea lavas fall on a horizontal trend with no obvious difference in Fe/Mn with increasing SiO_2* content. Ko'olau lavas have higher SiO_2* content than Kilauea lavas, but Ko'olau lavas have similar or lower Fe/Mn than Kilauea lavas. Partial melts of garnet peridotite (Walter, 1998) are also plotted for comparison. Fe/Mn is negatively correlated with SiO_2 content in partial melts of garnet peridotite, and Hawaiian lavas have higher Fe/Mn than these partial melts of garnet peridotite.

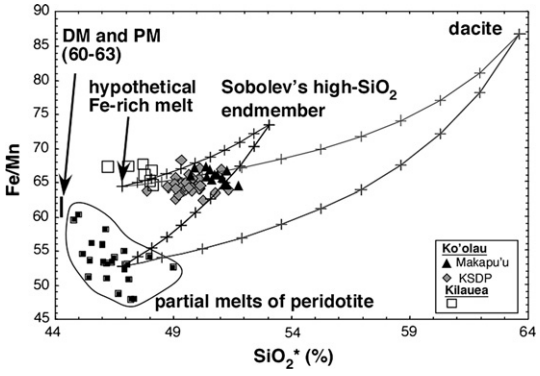

Fig. 8. SiO_2* versus Fe/Mn in Ko'olau and Kilauea lavas. Since Fe/Mn is not very sensitive to olivine fractionation and accumulation (see Kilauea lavas in Fig. 2), we use the measured Fe/Mn in this figure. Mixing trends between two picrite endmembers and SiO_2-rich endmembers proposed by Huang and Frey (2005) and Sobolev et al. (2005, 2007) are shown. The endmember compositions are given in Table 3. See text for details. The mixing increment is 10%. Fe/Mn in depleted mantle (DM) and primitive mantle (PM) (McDonough and Sun, 1995; Salters and Stracke, 2004 and Workman and Hart, 2005) are shown for comparison. Partial melts of peridotite are from Walter (1998).

The model of Sobolev et al. (2005, 2007) proposed that Hawaiian shield lavas are mixtures of partial melts derived from secondary garnet pyroxenite and peridotite; the proportion of melt derived from secondary garnet pyroxenite varies from ~30% in Kilauea lavas to >90% in Makapu'u-stage Ko'olau lavas. Two mixing lines in Fig. 8 show the effect of the high SiO_2 melt of the secondary garnet pyroxenite on Fe/Mn of the mixtures (Table 3). Two picritic melt compositions are used in the modeling: the average composition of partial melts of garnet peridotite at 3–4 GPa, which has Fe/Mn of 53 (Walter, 1998; Table 3), and a hypothetical picritic melt of Fe-rich garnet peridotite, which has Fe/Mn of 64, similar to those in Hawaiian lavas (Fig. 8). Sobolev et al. (2007) proposed that the high SiO_2 endmember in Hawaiian lavas have 53% SiO_2, 8% FeO, and Fe/Mn of 73 (Table 3). The mixing line between this high SiO_2 endmember and the picritic melt with Fe/Mn of 53 is nearly straight. Although this mixing line can reproduce the high Fe/Mn observed in some Ko'olau lavas, it significantly underestimates the Fe/Mn in Kilauea lavas, which have Fe/Mn similar to, or higher than, Ko'olau lavas (Fig. 8). In addition, this mixing model predicts that the Fe/Mn of Hawaiian shield lavas varies from ~52 to 61 as observed in MORB and Icelandic picrites (Qin and Humayun, submitted for publication) to high values (~70) as a function of the amount of partial melt from the secondary garnet pyroxenite. This is not observed, but to the contrary some KSDP Ko'olau lavas exhibit Fe/Mn lower than that of Kilauea lavas (Figs. 2 and 8).

Similarly, the mixing line between the high SiO_2 endmember in the model of Sobolev et al. (2005, 2007) and the hypothetical picritic melt of Fe-rich peridotite with Fe/Mn of 64 is also nearly straight, and at high SiO_2* this mixing line trends above the nearly horizontal Hawaiian trend (Fig. 8). Therefore, the nearly constant Fe/Mn in Hawaiian lavas is not consistent with mixing melts derived from the secondary garnet pyroxenite as proposed by Sobolev et al. (2005, 2007).

On the other hand, although the dacite melt has very high Fe/Mn (up to 87), it has very low FeO (5%), and MnO (0.06%) contents (e.g., Pertermann and Hirschmann, 2003; Table 3). Consequently, mixing lines between picrite melts and a dacite melt are hyperbolic, curving upwards to high SiO_2 (Fig. 8). The mixing line involving the picrite melt with Fe/Mn of 53 plots below the nearly horizontal Hawaiian trend. But the mixing line involving the hypothetical Fe-rich picrite melt, with Fe/Mn of 64, reproduces the nearly horizontal Hawaiian trend. Adding up to 30% dacite melt only increases Fe/Mn from 64 to 67. This effect is also

shown in Fig. 4, that is the lower MnO contents in Ko'olau lavas are accompanied by lower total Fe_2O_3 contents, so the net result is that Ko'olau lavas have Fe/Mn similar to those in Kilauea lavas (Figs. 2 and 8). Therefore, we suggest that the high Fe/Mn in Hawaiian lavas arises from the high-MgO, low-SiO_2 picritic endmember in Hawaiian lavas, which must then reflect a mantle source signature. The presence of high Fe/Mn mantle source beneath Hawaii may be accounted for by core-mantle interaction (Humayun et al., 2004), or by other possibilities. Although the mechanism proposed by Sobolev et al. (2005, 2007) does not explain the bulk of Ko'olau data (Fig. 8), it may be relevant at other Hawaiian volcanoes. For example, Herzberg (2006) proposed that both high-SiO_2 and low-SiO_2 groups tholeiitic lavas at Mauna Kea are partial melts of secondary garnet pyroxenites (Sobolev et al., 2005, 2007), a proposal that remains to be tested using Fe/Mn and MnO content.

4.4. Sampling eclogite in the Hawaiian plume

There is no doubt that the geochemical characteristics of Ko'olau lavas (Makapu'u and KSDP lavas), and of Hawaiian shield lavas in general, reflect mixing of SiO_2-rich and SiO_2-poor endmembers. Hauri (1996) and Huang and Frey (2005) proposed that the SiO_2-rich Ko'olau endmember is a high-SiO_2, low-MgO dacite endmember, formed by low degree (10–20%) partial melting of eclogite. Pertermann and Hirschmann (2003) suggested that the SiO_2-rich Ko'olau (Makapu'u) endmember is andesite or basaltic andesite, which are moderate degree partial melts of eclogite. In contrast, Sobolev et al. (2005) proposed that the Ko'olau endmember is a high-SiO_2, high-MgO melt, generated by moderate degree (~40%) partial melting of a secondary garnet pyroxenite. Can these models be distinguished?

The measured MnO contents in Ko'olau lavas are correlated with SiO_2*, MgO*, and $(Na_2O + K_2O)$* contents, and Al_2O_3/CaO (Fig. 6). The positive MgO*-MnO trend (Fig. 6b) of Ko'olau lavas points to the low-MgO (<5%) and MnO part of the partial melt trend of eclogite, which is consistent with the SiO_2-rich Ko'olau (Makapu'u) endmember being dacite or low-MgO andesite but not basaltic andesite. Supporting this inference, based on MgO*–SiO_2* correlation of Ko'olau lavas, Huang and Frey (2005) inferred that the SiO_2-rich endmember in Ko'olau lavas has ~66% SiO_2 and ~2% MgO. The trends in Fig. 6 define mixing lines between picritic melts derived from peridotite (Walter, 1998) and dacite or low-MgO andesite melts derived from eclogite (Pertermann and Hirschmann, 2003).

Although the experimental partial melts of a secondary garnet pyroxenite (Sobolev et al., 2007) are also on the extension of the Ko'olau trend in the plots of SiO_2* and MgO* vs MnO (Figs. 6a and b), these experimental melts are offset from the Ko'olau trends to lower MnO content (<0.13%) in the plots of $(Na_2O + K_2O)$* and Al_2O_3/CaO vs MnO (Figs. 6c and d). The $Na_2O + K_2O$ content in the starting pyroxenite composition of Sobolev et al. (2007) could be adjusted upwards if the dacite melt involved in the first stage of the Sobolev et al. (2005) model is more enriched in $Na_2O + K_2O$, e.g., if this dacite melt was a low degree (10–20%) partial melt formed from oceanic crust instead of gabbroic crust (Table S2 of Sobolev et al., 2005). However, the Al_2O_3/CaO–MnO plot is more robust (Fig. 6d). The Al_2O_3/CaO ratio in partial melts of garnet peridotite is pressure dependant. At 3–4 GPa partial melts of garnet peridotite have Al_2O_3/CaO of 1.2 ± 0.1, similar to those of the fertile peridotites used as the starting compositions (Walter, 1998). A mixing line between partial melts of garnet peridotite at 3–4 GPa and a dacite melt is nearly straight, and it explains the Al_2O_3/CaO–MnO trend in Ko'olau lavas (Fig. 6d). However, partial melts of the secondary garnet pyroxenite have Al_2O_3/CaO of 1.5–1.9, similar to or greater than those of Makapu'u-stage Ko'olau lavas, but at significantly lower MnO content (<0.13% vs >0.15%). The secondary garnet peridotite used in Sobolev et al. (2007) has Al_2O_3/CaO of 1.6, and the alternative secondary garnet pyroxenite proposed by Sobolev et al. (2005) has Al_2O_3/CaO of 1.8. In the model of Sobolev et al. (2005) the Makapu'u-stage Ko'olau lavas represent nearly pure melts of the secondary garnet pyroxenite, while most other Hawaiian shield lavas are explained as mixtures of melts derived from peridotite and secondary garnet pyroxenite. It can be seen from Fig. 6d that this model predicts MnO content too low to explain the MnO content (0.15–0.18%) of Ko'olau lavas. Therefore, we argue that the high-SiO_2 Ko'olau (Makapu'u) endmember is consistent with a dacite or low-MgO andesite melt, but not with a partial melt derived from secondary garnet pyroxenite.

Based on the "sandwich"-type experiments of Yaxley and Green (1998), it is expected that SiO_2-rich dacite melt from eclogite reacts with surrounding peridotite to form secondary garnet pyroxenite (e.g., Sobolev et al., 2005). Our geochemical data for Ko'olau lavas appear to be in conflict with this expectation since we propose mixing between picrite melt derived from peridotite with dacite (or low-MgO andesite) melt derived from eclogite. Sobolev et al. (2005) depicted eclogite as pods surrounded by peridotite; in this physical context dacite melt derived from eclogite is likely to react with the surrounding peridotite. However recent models for the geometry of mantle heterogeneities beneath Hawaii have indicated that compositional heterogeneities, such as eclogite, are stretched into long filaments, laterally continuous over tens or hundreds of kilometers (Farnetani et al., 2002; Farnetani and Samuel, 2005). Lead isotope evidence for such filaments, termed "spaghetti", can be found in the long-term persistence of the "Loa" and "Kea" geochemical trends (Abouchami et al., 2005). Like the model proposed by Abouchami et al. (2005), we propose that this physical context applies to entrained oceanic crust (eclogite) in the Hawaiian plume. If the eclogite was present as long filaments parallel to the plume axis laterally continuous over tens or hundreds of kilometers, then dacite melt could travel through the eclogite matrix towards the surface without substantial reaction with peridotite.

5. CONCLUSIONS

A precise method for obtaining Fe/Mn ratios and MnO contents has been used to analyze lavas forming the Hawaiian shields of Ko'olau and Kilauea. The Fe/Mn of unaltered

Ko'olau lavas ranges from 62.7 to 68.4, and the Fe/Mn of Kilauea lavas ranges from 64.6 to 67.7. The MnO ranges are narrow: 0.156–0.176% in KSDP Ko'olau lavas; 0.146–0.160% in Makapuu-stage Ko'olau lavas; and 0.166–0.174% in Kilauea lavas. These MnO ranges are small compared with the uncertainties of MnO data obtained by traditional analytical techniques such as XRF and electron microprobe. Our more precise MnO data show that the MnO contents of Ko'olau lavas are correlated with Nd–Hf–Pb isotopic ratios, La/Nb and Al_2O_3/CaO, and olivine-adjusted contents of SiO_2, MgO and $Na_2O + K_2O$, thereby implying two-endmember mixing. These correlations show that the enriched Hawaiian endmember, the Ko'olau (Makapu'u) endmember, is characterized by high SiO_2, $Na_2O + K_2O$ and Al_2O_3/CaO, and low MgO and MnO. There are no known means of generating this SiO_2-rich, MnO-poor endmember by partial melting of garnet peridotite, without the involvement of eclogite. Rather, the high SiO_2, low MnO Ko'olau (Makapu'u) endmember can be a dacite or low-MgO andesite melt, formed by low degree (10–20%) partial melting of eclogite.

The involvement of dacite (or low-MgO andesite) melt does not explain the observed high Fe/Mn in Hawaiian shield lavas because dacite melt has FeO and MnO contents too low to significantly increase the Fe/Mn in the mixed magmas. Further, the lack of correlation between Fe/Mn and olivine-adjusted SiO_2 content in Hawaiian lavas is inconsistent with the two-stage partial melting of eclogite model proposed by Sobolev et al. (2005, 2007). We argue that the high Fe/Mn of Hawaiian lavas originates from the picrite endmember. Variable addition of dacite melt to this picritic melt explains the systematic correlation of MnO content with major element contents and ratios, trace element ratios and radiogenic isotopic ratios observed in Ko'olau lavas. The origin of the high Fe/Mn in the mantle beneath Hawaii may be due to core-mantle interaction (as previously proposed) or to other processes.

ACKNOWLEDGMENTS

We thank T. Zateslo for maintaining the Element at FSU. We thank M. Bizimis, C. Herzberg, M. Norman, and V.J.M. Salters for discussions, and M. Hirschmann, A. Scherstén, and an anonymous referee for constructive reviews. We thank M. Rehkämper for editorial handling. Support by NSF EAR-0509176 is gratefully acknowledged.

REFERENCES

Abouchami W., Hofmann A. W., Galer S. J. G., Frey F. A., Eisele J. and Feigenson M. (2005) Lead isotopes reveal bilateral asymmetry and vertical continuity in the Hawaiian mantle plume. *Nature* **434**, 851–856. doi:10.1038/nature03402.

Beattie P. (1994) Systematics and energetics of trace-element partitioning between olivine and silicate melts: Implications for the nature of mineral/melt partitioning. *Chem. Geol.* **117**, 57–71. doi:10.1016/0009-2541(94)90121-X.

Bennett V. C., Esat T. M. and Norman M. D. (1996) Two mantle-plume components in Hawaiian picrites inferred from correlated Os–Pb isotopes. *Nature* **381**, 221–224.

Blichert-Toft J., Frey F. A. and Albarede F. (1999) Hf isotope evidence for pelagic sediments in the source of Hawaiian basalts. *Science* **285**(5429), 879–882.

Brandon A. D., Norman M. D., Walker R. J. and Morgan J. W. (1999) ^{186}Os–^{187}Os systematics of Hawaiian picrites. *Earth Planet. Sci. Lett.* **172**, 25–42.

Chen C.-Y., Frey F. A., Rhodes J. M. and Easton R. M. (1996) Temporal geochemical evolution of Kilauea Volcano: comparison of Hilina and Puna Basalt. In *Earth Processes: Reading the Isotopic Code*, 95 (eds. A. Basu and S. R. Hart), pp. 161–181. Geophysical Monograph Series. AGU, Washington, DC.

Decker, R.W., Wright, T.L. and Stauffer, P.H. (1987) Volcanism in Hawaii: U.S. Geological Survey Professional Paper 1350.

Eggins S. M. (1992) Petrogenesis of Hawaiian tholeiites; 1, phase equilibria constraints. *Contrib. Mineral. Petrol.* **110**(2-3), 387–397.

Ewart A. and Griffin W. L. (1994) Application of proton-microprobe data to trace-element partitioning in volcanic-rocks. *Chem. Geol.* **117**(1–4), 251–284. doi:10.1016/0009-254(94)90131-7.

Farnetani C. G., Legras B. and Tackley P. J. (2002) Mixing and deformations in mantle plumes. *Earth Planet Sci. Lett.* **196**(1–2), 1–15.

Farnetani C. G. and Samuel H. (2005) Beyond the thermal plume paradigm. *Geophys. Res. Lett.* **32**, L07311. doi:10.1029/2005GL022360.

Feigenson M. D., Hofmann A. W. and Spera F. J. (1983) Case studies on the origin of basalt. II. The transition from tholeiitic to alkalic volcanism on Kohala volcano, Hawaii. *Contrib. Mineral. Petrol.* **84**, 390–405.

Fekiacova, Z., Abouchami, W., Galer, S.J.G., Garcia, M.O. and Hofmann, A.W. (2007) Temporal evolution of Ko'olau Volcano: inferences from isotope results on the Ko'olau Scientific Drilling Project (KSDP) and Honolulu Volcanics, Earth Planet Sci. Lett., in press.

Forte A. M. and Mitrovica J. X. (2001) Deep mantle high viscosity flow and thermochemical structure inferred from seismic and geodynamic data. *Nature* **410**, 1049–1056.

Frey F. A., Garcia M. O., Wise W. S., Kennedy A., Gurriet P. and Albarede F. (1991) The evolution of Mauna Kea volcano, Hawaii: petrogenesis of tholeiitic and alkalic basalts. *J. Geophys. Res.* **96**, 14,347–14,375.

Frey F. A. and Rhodes J. M. (1993) Inter-shield geochemical differences among Hawaiian volcanoes: implications for source compositions, melting processes and magma ascent paths. *Philos. Trans. R. Soc. Lond. A* **342**, 121–136.

Frey F. A., Garcia M. O. and Roden M. F. (1994) Geochemical characteristics of Koolau Volcano: implications of intershield geochemical differences among Hawaiian volcanoes. *Geochim. Cosmochim. Acta* **58**, 1441–1462.

Galer S. J. G. and O'Nions R. K. (1985) Residence time of thorium, uranium and lead in the mantle with implications for mantle convection. *Nature* **316**, 778–782.

Garcia M. O. (2002) Submarine picritic basalts from Ko'olau Volcano, Hawai'i: implications for parental magma compositions and mantle source. In *Hawaiian Volcanoes; Deep Underwater Perspectives*, 128 (eds. E. Takahashi, P. W. Lipman, M. O. Garcia, J. Naka and S. Aramaki), pp. 391–401. Geophysical Monograph Series.

Haskins E. R. and Garcia M. O. (2004) Scientific drilling reveals geochemical heterogeneity within the Ko'olau shield, Hawai'i. *Contrib. Mineral. Petrol.* **147**, 162–188.

Hauri E. H. (1996) Major-element variability in the Hawaiian mantle plume. *Nature* **382**, 415–419.

Herzberg C. (2006) Petrology and thermal structure of the Hawaiian plume from Mauna Kea volcano. *Nature* **444**, 605–609. doi:10.1038/nature05254.

Huang S. and Frey F. A. (2003) Trace element abundances of Mauna Kea basalt from Phase 2 of the Hawaiian Scientific Drilling Project: Petrogenetic implications of correlations with major element content and isotopic ratios. *Geochem. Geophys. Geosyst.* **4**(6), 8711. doi:10.1029/2002GC000322.

Huang S. and Frey F. A. (2005) Recycled oceanic crust in the Hawaiian Plume: evidence from temporal geochemical variations within the Koolau shield. *Contrib. Mineral. Petrol.* **149**, 556–575. doi:10.1007/s00410-005-0664-9.

Huang S., Frey F. A., Blichert-Toft J., Fodor R. V., Bauer G. R. and Xu G. (2005) Enriched components in the Hawaiian plume: evidence from Kahoolawe Volcano, Hawai'i. *Geochem. Geophys. Geosyst.* **6**, Q11006. doi:10.1029/2005GC001012.

Humayun M., Qin L. and Norman M. D. (2004) Geochemical evidence for excess iron in the mantle beneath Hawai'i. *Science* **306**, 91–94.

Hirose K. and Kushiro I. (1993) Partial melting of dry peridotites at high pressures: determination of compositions of melts segregated from peridotite using aggregated diamond. *Earth Planet Sci. Lett.* **114**, 477–489.

Lassiter J. C., DePaolo D. J. and Tatsumoto M. (1996) Isotopic evolution of Muana Kea Volcano: results from the initial phase of the Hawaiian Scientific Drilling Project. *J. Geophys. Res.* **101**, 11,769–11,780.

Lassiter J. C. and Hauri E. H. (1998) Osmium-isotope variations in Hawaiian lavas: evidence for recycled oceanic lithosphere in the Hawaiian plume. *Earth Planet Sci Lett.* **164**, 483–496.

Li X., Kind R., Yuan X., Wölbern I. and Hanka W. (2004) Rejuvenation of the lithosphere by the Hawaiian plume. *Nature* **427**, 827–829. doi:10.1038/nature02349.

McDonough W. F. and Sun S.-s. (1995) The composition of the Earth. *Chem. Geol.* **120**, 223–253.

Nielsen S. G., Rehkämper M., Norman M. D., Halliday A. N. and Harrison D. (2006) Thallium isotopic evidence for ferromanganese sediments in the mantle source of Hawaiian basalts. *Nature* **439**, 314–317. doi:10.1038/nature04459.

Norman M. D. and Garcia M. O. (1999) Primitive magmas and source characteristics of the Hawaiian Plume; petrology and geochemistry of shield picrites. *Earth Planet Sci. Lett.* **168**, 27–44.

Pertermann M. and Hirschmann M. M. (2003) Anhydrous partial melting experiments on MORB-like eclogite: phase reactions, phase compositions and mineral-melt partitioning of major elements at 2–3 GPa. *J. Petrol.* **44**(12), 2173–2201.

Pertermann M., Hirschmann M. M., Hametner K., Gunther D. and Schmidt M. W. (2004) Experimental determination of trace element partitioning between garnet and silica-rich liquid during anhydrous partial melting of MORB-like eclogite. *Geochem. Geophys. Geosyst.* **5**, Q05A01. doi:10.1029/2003GC000638.

Qin, L. and Humayun, M, The Fe/Mn ratio in MORB and OIB determined by ICP-MS. *Geochim. Cosmochim. Acta.*, submitted for publication.

Ravizza G., Blusztajn J. and Prichard H. M. (2001) Re–Os systematics and platinum-group element distribution in metalliferous sediments from the Troodos ophiolite. *Earth Planet Sci. Lett.* **188**, 369–381.

Ren Z.-Y., Ingle S., Takahashi E., Hirano N. and Hirata T. (2005) The chemical structure of the Hawaiian mantle plume. *Nature* **436**, 837–840. doi:10.1038/nature03907.

Rhodes J. M. (1996) Geochemical stratigraphy of lava flows sampled by the Hawai'i Scientific Drilling Project. *J. Geophys. Res.* **101**, 11,729–11,746.

Rhodes J. M. and Vollinger M. J. (2004) Composition of basaltic lavas sampled by phase-2 of the Hawai'i Scientific Drilling Project: geochemical stratigraphy and magma types. *Geochem. Geophys. Geosyst.* **5**, Q03G13. doi:10.1029/2002GC000434.

Roden M. F., Trull T., Hart S. R. and Frey F. A. (1994) New He, Sr, Nd and Pb isotopic constraints on the constitution of the Hawaiian plume: Results from Koolau Volcano, Oahu, Hawaii. *Geochim. Cosmochim. Acta.* **58**, 1431–1440.

Salters V. J. M. and Stracke A. (2004) The composition of the depleted mantle. *Geochem. Geophys. Geosyst.* **5**(5). doi:10.1029/2003GC000597.

Salters V. J. M., Blichert J., Fekiacova Z., Sachi-Kocher A. and Bizimis M. (2006) Isotope and trace element evidence for depleted lithosphere in the source of enriched Koolau basalts. *Contrib. Mineral. Petrol.* **151**, 297–312. doi:10.1007/s00410-005-0059-y.

Sobolev A. V., Hofmann A. W., Sobolev S. V. and Nikogosian I. K. (2005) An olivine free mantle source of Hawaiian shield basalts. *Nature* **434**, 590–597. doi:10.1038/nature03411.

Sobolev A. V., Hofmann A. W., Kuzmin D. V., Yaxley G. M., Arndt N. T., Chung S-. L., Garcia M. O., Gurenko A. A., Danyushevsky L. V., Elliott T., Frey F. A., Kamenetsky V. S., Kerr A. C., Krivolutskaya N. A., Matvienkov V. V., Nikogosian I. K., Rocholl A., Suschevskaya N. M. and Teklay M. (2007) The amount of recycled crust in sources of mantle-derived melts. *Science* **316**, 412–417. doi:10.1126/science.1138113.

Stolper E., Sherman S., Garcia M., Baker M. and Seaman C. (2004) Glass in the submarine section of the HSDP2 drill core, Hilo, Hawai'i. *Geochem. Geophys. Geosyst.* **5**, Q07G15. doi:10.1029/2003GC000553.

Stracke A., Salters V. J. M. and Sims K. W. W. (1999) Assessing the presence of garnet–pyroxenite in the mantle sources of basalts through combined hafnium–neodymium–thorium isotope systematics. *Geochem. Geophys. Geosyst.* **1**, paper #1999000013.

Takahashi E. and Nakajima K. (2002) Melting process in the Hawaiian Plume; an experimental study. In *Hawaiian volcanoes; deep underwater perspectives*, 128 (eds. E. Takahashi, P. W. Lipman, M. O. Garcia, J. Naka and S. Aramaki), pp. 403–418. Geophysical Monograph Series.

Wagner T. P. and Grove T. L. (1998) Melt/harzburgite reaction in the petrogenesis of tholeiitic magma from Kilauea Volcano, Hawai'i. *Contrib. Mineral. Petrol.* **131**(1), 1–12.

Walter M. J. (1998) Melting of garnet peridotite and the origin of komatiite and depleted lithosphere. *J. Petrol.* **39**(1), 29–60.

Workman R. K. and Hart S. R. (2005) Major and trace element composition of the depleted MORB mantle (DM). *Earth Planet Sci. Lett.* **231**, 53–72. doi:10.1016/j.epsl.2004.12.005.

Yang H.-J., Frey F. A., Rhodes J. M. and Garcia M. O. (1996) Evolution of Mauna Kea volcano: inferences from lava compositions recovered in the Hawai'i Scientific Drilling Project. *J. Geophys. Res.* **101**, 11,747–11,767.

Yaxley G. M. and Green D. H. (1998) Reactions between eclogite and peridotite: mantle refertilisation by subduction of oceanic crust. *Schweiz. Mineral. Petrogr. Mitt.* **78**, 243–255.

Yogodzinski G. M., Kay R. W., Volynets O. N., Koloskov A. V. and Kay S. M. (1995) Magnesian andesite in the western Aleutian Komandorsky region; implications for slab melting and processes in the mantle wedge. *Geol. Soc. Am. Bull.* **107**(5), 505–519.

Associate editor: Mark Rehkamper